

Fast numerical method for the Boltzmann equation on non-uniform grids

Alexei Heintz^a, Piotr Kowalczyk^{b,*}, Richards Grzhibovskis^c

^a Department of Mathematics, Chalmers University of Technology and Göteborg University, SE-412 96 Göteborg, Sweden

^b Institute of Applied Mathematics and Mechanics, University of Warsaw, Banacha 2, 02-097 Warszawa, Poland

^c FR 6.1 Mathematik, Universität des Saarlandes, Postfach 151150, 66041 Saarbrücken, Germany

Received 25 May 2007; received in revised form 27 December 2007; accepted 23 March 2008

Available online 31 March 2008

Abstract

We introduce a new fast numerical method for computing discontinuous solutions to the Boltzmann equation and illustrate it by numerical examples. A combination of adaptive grids for approximation of the distribution function and an approximate fast Fourier transform on non-uniform grids for computing smooth terms in the Boltzmann collision integral is used.

© 2008 Elsevier Inc. All rights reserved.

Keywords: Boltzmann equation; Numerical methods; Non-uniform grids

1. Introduction

This paper is devoted to a new deterministic scheme for numerical solution of the classical *Boltzmann equation* [10] for a dilute gas of particles

$$\frac{\partial f}{\partial t} = Q(f, f), \quad (1)$$

where $f := f(t, \mathbf{v})$ and $f : \mathbb{R}_+ \times \mathbb{R}^3 \rightarrow \mathbb{R}_+$. We concentrate mainly on a new approach to the approximation of the collision operator $Q(f, f)$ for distribution functions f discontinuous in velocity space and demonstrate the method on the space homogeneous equation (1).

The collision operator $Q(f, f)$ for molecular potentials with angular cut off [10] can be decomposed into the *gain* and the *loss* parts:

* Corresponding author.

E-mail addresses: heintz@math.chalmers.se (A. Heintz), pkowal@mimuw.edu.pl (P. Kowalczyk), richards@num.uni-sb.de (R. Grzhibovskis).

$$\mathcal{Q}(f, f)(\mathbf{v}) = \mathcal{Q}^+(f, f)(\mathbf{v}) - \mathcal{Q}^-(f, f)(\mathbf{v}), \quad (2)$$

$$\mathcal{Q}^+(f, f)(\mathbf{v}) = \int_{\mathbb{R}^3} \int_{S^2} B(|\mathbf{u}|, \theta) f\left(\mathbf{v} - \frac{1}{2}(\mathbf{u} - |\mathbf{u}|\omega)\right) f\left(\mathbf{v} - \frac{1}{2}(\mathbf{u} + |\mathbf{u}|\omega)\right) d\omega d\mathbf{u} \quad (3)$$

and

$$\mathcal{Q}^-(f, f)(\mathbf{v}) = f(\mathbf{v})q^-(f)(\mathbf{v}) \quad (4)$$

with q^- denoting the collision frequency term

$$q^-(f)(\mathbf{v}) = \int_{\mathbb{R}^3} f(\mathbf{v} - \mathbf{u}) \int_{S^2} B(|\mathbf{u}|, \theta) d\omega d\mathbf{u}.$$

The function $B(|\mathbf{u}|, \theta)$ is of the form

$$B(|\mathbf{u}|, \theta) = B_0\left(|\mathbf{u}|, \frac{|(\mathbf{u}, \omega)|}{|\mathbf{u}|}\right), \quad \mathbf{u} \in \mathbb{R}^3, \quad \omega \in S^2, \quad S^2 = \{\mathbf{q} \in \mathbb{R}^3 : |\mathbf{q}| = 1\}.$$

It contains the information about the binary interactions of particles and reflects the physical properties of the model. In the case of a popular Variable Hard Sphere (VHS) model [3] the collision kernel B has the following form:

$$B(|\mathbf{v} - \mathbf{w}|, \theta) = C_\alpha |\mathbf{v} - \mathbf{w}|^\alpha \quad (5)$$

with $-3 < \alpha \leq 1$. For $\alpha = 0$ with $C_0 = \frac{1}{4\pi}$ we get the so called Maxwellian gas and for $\alpha = 1$ with $C_1 = 1$ we get the gas of “hard sphere” molecules.

We will use the following form of the Fourier transform:

$$\mathcal{F}_v(\mathbf{m})[f] := \hat{f}_{\mathbf{m}} = \int_{\mathbb{R}^3} f(\mathbf{v}) e^{2\pi i(\mathbf{v}, \mathbf{m})} d\mathbf{v} \quad (6)$$

and the inverse Fourier transform

$$\mathcal{F}_m^{-1}(\mathbf{v})[\hat{f}] := f(\mathbf{v}) = \int_{\mathbb{R}^3} \hat{f}_{\mathbf{m}} e^{-2\pi i(\mathbf{m}, \mathbf{v})} d\mathbf{m}. \quad (7)$$

One can reformulate the gain and the collision frequency terms using the Fourier transform:

$$\mathcal{Q}^+(f, f)(\mathbf{v}) = \mathcal{F}_l^{-1}(\mathbf{v}) \mathcal{F}_m^{-1}(\mathbf{v}) [\hat{f}_{\mathbf{l}} \hat{f}_{\mathbf{m}} \hat{B}(\mathbf{l}, \mathbf{m})], \quad (8)$$

$$q^-(f)(\mathbf{v}) = \mathcal{F}_m^{-1}(\mathbf{v}) [\hat{f}_{\mathbf{m}} \hat{B}(\mathbf{m}, \mathbf{m})], \quad (9)$$

where

$$\hat{B}(\mathbf{l}, \mathbf{m}) = \int_{\mathbb{R}^3} \int_{S^2} B(|\mathbf{u}|, \theta) e^{2\pi i(\frac{\mathbf{l}+\mathbf{m}}{2}, \mathbf{u})} e^{2\pi i|\mathbf{u}|(\frac{\mathbf{m}-\mathbf{l}}{2}, \omega)} d\omega d\mathbf{u}. \quad (10)$$

The gain term is a kind of bilinear pseudo-differential operator with symbol $\hat{B}(\mathbf{l}, \mathbf{m})$. The kernel $\hat{B}(\mathbf{l}, \mathbf{m})$ is a distribution, hence in order to use it in practical computations one has to regularize it. By choosing a proper constant $R > 0$ one can write the regularized kernel as [23]

$$\hat{B}_R(\mathbf{l}, \mathbf{m}) = \int_{B(0, R)} \int_{S^2} B(|\mathbf{u}|, \theta) e^{2\pi i(\frac{\mathbf{l}+\mathbf{m}}{2}, \mathbf{u})} e^{2\pi i|\mathbf{u}|(\frac{\mathbf{m}-\mathbf{l}}{2}, \omega)} d\omega d\mathbf{u}. \quad (11)$$

We denote by $\mathcal{Q}_R^+(f, f)$ and $q_R^-(f)$ the gain and collision frequency terms with the regularized kernel \hat{B}_R . The kernel \hat{B}_R can be computed analytically for the hard sphere gas and for the Maxwell gas (see [23]). We use the explicit formulas for \hat{B}_R from [23] later in our computations.

The major part of applied computations concerning the Boltzmann equation is based on various variants of the probabilistic Monte Carlo methods, see [4,24]. The development of deterministic methods for the Boltzmann equation is usually motivated, see [23,19], by the desire of higher precision results in situations when probabilistic methods are not effective enough.

Several different ideas led to various types of discrete velocity models (DVM) satisfying exact conservation laws in discrete form [12,25,9,21]. Also rigorous consistency and convergence results for such models were proved [20,17,21]. All above mentioned DVM methods have high computational cost of order n^7 with n denoting here the number of points along one coordinate direction in the uniform velocity grid. Another disadvantage is that the integration over the sphere S^2 of the possible outputs of collisions in $Q(f, f)$ is approximated with low precision [20,21] in DVM.

The Kyoto group in kinetic theory has developed a family of finite difference methods for the Boltzmann equation, linearized Boltzmann equation and the BGK equation and investigated numerically many mostly stationary problems [19,13]. These computations demonstrate precise results but they are very time and memory consuming.

Applying Fourier transform to the Boltzmann collision operator leads to essential simplifications in the case of Maxwell pseudo-molecules [7]. Using this reduction and the fast Fourier transform (FFT) led authors of [11,5] to a fast deterministic method restricted to Maxwell pseudo-molecules and having low computational cost $O(N^4)$ and accuracy $O(1/\sqrt{N})$. Here N is the number of Fourier modes along one coordinate direction. Another method designed for the model of hard spheres and also using FFT was suggested in [8] and has computational cost $N^6 \log N$ and a higher accuracy of order $1/N^2$. A spectral method based on the restriction of the Boltzmann equation to a finite domain and on the representation of the solution by Fourier series was suggested in [22] and developed further in [23]. This method has an advantage of high spectral accuracy for smooth solutions to the Boltzmann equation and complexity $O(N^6)$.

The main goal of the present paper is to design a Fourier based deterministic method for computation of the collision operator $Q(f, f)$ with discontinuous distribution functions f . We also apply it to space homogeneous problems with discontinuous initial data for Maxwell pseudo-molecules and for hard sphere molecules. We are interested in discontinuous solutions because they are typical for flows around a body. It is particularly easy to observe in regimes close to collisionless. Computations done by the Kyoto group show that discontinuous distribution functions are typical for flows around bodies for a wide range of Knudsen numbers [26].

Using Fourier transform for computation of $Q(f, f)$ is attractive because one goes around the integration over the sphere in (2) and makes use of the convolution structure in $Q(f, f)$. But Fourier based spectral approximations for discontinuous solutions lose accuracy because of the Gibbs phenomenon.

The main idea here is to combine an adaptive approximation for discontinuous solutions f to the Boltzmann equation with Fourier spectral approximation for the smooth terms in the equation: the gain term $Q^+(f, f)$ and the collision frequency $q^-(f)$. It is based on the classical result that in the case of Maxwell molecules and hard potentials with cut off the gain term $Q^+(f, f)$ in the collision operator has certain smoothing properties and is actually smooth even for a discontinuous f . This property was found first in [16] and later investigated in details in [27,18]. The collision frequency $q^-(f)$ is also a smooth function because it is a convolution of f with a regular function. A detailed study of the propagation of smoothness and singularity of solutions was done in [18]. These results give a theoretical motivation to our numerical approach. To illustrate the smoothing properties of $Q^+(f, f)$ we give here a numerical example with the graph of $Q^+(f, f)$ in the x - y plane for a discontinuous function f in the case of hard sphere gas, see Fig. 1.

Discontinuous solutions to the space homogeneous Boltzmann equation are computed in the present paper by the following recursive algorithm:

- (1) Building of an adaptive grid starts with a coarse uniform grid over a cube. Values of the distribution function f in the centres of the cubes in the grid are calculated. At the initial time f is given analytically, at the next time steps it is computed as it is described in (5) below.
- (2) We identify the cubes where the variation of f over neighbouring cubes is larger than a desired precision. All such cubes are divided into eight similar cubes and the solution f is computed in the centres of the new cubes that appeared after the subdivision. This procedure is repeated again for all new cubes until the minimal grid step is reached or the variation of f is smaller than the desired precision. A new adaptive grid is ready.
- (3) A moderately small amount of Fourier coefficients for f given on the non-uniform grid is computed using an approximate fast Fourier transform by Beylkin [2].
- (4) Fourier coefficients for smooth terms $Q^+(f, f)$ and $q^-(f)$ in the Boltzmann equation are computed.
- (5) We compute f at the next time step by an explicit Runge–Kutta method. Then we go to (2) and build a new adaptive grid for f . In these computations we use the values of f at the previous time step and the corresponding Fourier spectral representation for the smooth terms $Q^+(f, f)$ and $q^-(f)$ in the Boltz-

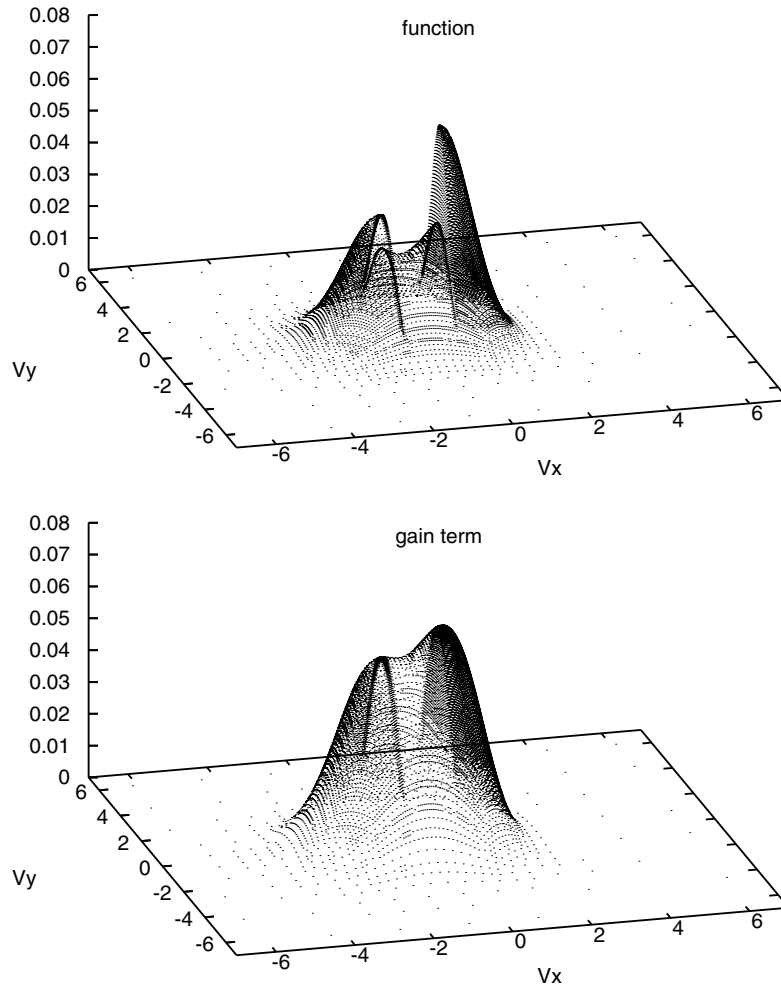


Fig. 1. Distribution function f with discontinuity and the corresponding gain term $Q^+(f, f)$.

mann equation. We apply again the approximate fast Fourier transform [2] now for computing $Q^+(f, f)$ and $q^-(f)$ on the new adaptive grid.

Details of the computations with the tests and the illustrative examples are described in the rest of the paper.

2. Discretization of the collision integral

2.1. Grid generation

We illustrate our approach to the numerical solution of the Boltzmann equation by the space homogeneous problems with discontinuous initial data. The distribution function $f(t, \mathbf{v})$ is usually negligible outside some ball, so for the numerical treatment of the Boltzmann equation we assume that $\text{supp } f \subset \Omega_v := [-L, L]^3$.

At each time step we build in a rather standard way a binary adaptive grid that follows the changes of the distribution function f in the cube Ω_v .

We start with some initial uniform coarse cubic grid, fix the desired precision and the minimal grid step we can accept. The values of the solution f in the centres of the cubes are computed. Then we identify those cubes for which the variation of f over centres of neighbouring cubes is larger than the desired precision. Each of these cubes with a side for example a is divided into eight similar small cubes with the side $a/2$. After the divi-

sion the values of f in the centres of the new small cubes are computed. At the initial time f is given analytically, at the next time steps it is computed by the method described later in the next sections. This dissection procedure is repeated recursively for each new generation of smaller cubes until the desired precision or the smallest accepted cube size is reached.

The resulting adaptive binary grid follows the variation of f in Ω_v being more dense around discontinuities and in regions with higher gradients. We illustrate it in Figs. 5 and 7 by showing centres of the cross-sections of the grid cubes by the coordinate plane $z = 0$ and the graphs for values of f at the same points in Figs. 4 and 6.

A new adaptive grid is created at each time step in parallel with the computation of the values of the solution at the next time step by an explicit Runge–Kutta finite difference scheme, that in turn uses a non-uniform fast Fourier spectral approximations for $Q_R^+(f, f)$ and $q_R^-(f)$, see Sections 3 and 2.3.

2.2. Discretization of Fourier transform

Now we focus on the numerical approximation of the Fourier transform integrals (6) and (7) for f defined on a non-regular grid. We restrict the function f to a bounded domain Ω_v . See [23] for a discussion of the validity of such a restriction. For the sake of simplicity we describe here the evaluation of the integral (6) for f approximated by a function \bar{f} piecewise constant on the cubic cells defined by the adaptive grid in the velocity space. The approach we use below does not depend much on this issue. We use below the notation \hat{f}_m for the Fourier transform of \bar{f} . An elementary integration implies

$$\hat{f}_m = \sum_K \bar{f}_K \int_K e^{2\pi i(\mathbf{v}, \mathbf{m})} d\mathbf{v} = \sum_K C_m \bar{f}_K \sum_{\mathbf{v}_K} \alpha_{\mathbf{v}_K} e^{2\pi i(\mathbf{v}_K, \mathbf{m})},$$

where K denotes a cubic cell of the adaptive grid in Ω_v with the vertices \mathbf{v}_K , \bar{f}_K is a constant approximating f on K , C_m is a constant depending only on \mathbf{m} and $\alpha_{\mathbf{v}_K} = \pm 1$. Collecting terms with exponents corresponding to the same vertex \mathbf{v}_j in the double sum above implies

$$\hat{f}_m = C_m \sum_j \bar{F}_j e^{2\pi i(\mathbf{v}_j, \mathbf{m})}, \tag{12}$$

where \bar{F}_j is a sum of contributions to the node \mathbf{v}_j of approximations \bar{f}_K from all cubes K having the node \mathbf{v}_j in common.

The standard fast Fourier transform (FFT) algorithm commonly used to compute numerically trigonometric sums cannot be used here for sums like one in (12), since the velocity points \mathbf{v}_j in Ω_v are not equidistant. To compute this sum effectively we use the *unequally spaced fast Fourier transform* (USFFT) algorithm developed by Beylkin [2]. This algorithm is formulated in [2] in such a way that the grid points \mathbf{v}_j lie within the cube $[-\frac{1}{2}, \frac{1}{2}]^3$. We scale our problem so the support of the function f lies in this cube.

The idea of the USFFT is that the sum of Fourier exponents with non-uniform nodes \mathbf{v}_j is interpreted as a Fourier transform of a linear combination of delta functions concentrated in these nodes. This linear combination of delta functions is projected on a subspace of B -splines of order p , usually $p \leq 5$. The Fourier transform of the projection is used as an approximation to the original sum of exponents. To get the inverse USFFT one does computations in the reverse order. First the projection of the function onto the subspace of B -splines is computed and then it is used to compute the function in arbitrary points. We give for completeness an outline of the particular algorithm we used (see [2]). Values of Fourier transform \hat{f}_m by formula (12) will be computed on a uniform grid in R^3 in a Fourier domain: $\{\mathbf{m} = (m_1, m_2, m_3) : m_1, m_2, m_3 = -M, \dots, M - 1\}$ for $M = 2^{-n-2}$ with $n < -2$. We will use for brevity the shortened notation $\mathbf{m} = -M, \dots, M - 1$ for multi-indices denoting points of such grids. Hence we need to compute the sum (12) for $\mathbf{m} = -M, \dots, M - 1$.

We let $N = 4M$. The first step is to compute the coefficients

$$g_k = \sum_j \bar{f}_j \beta_{k_1, n}^{(p)}(v_{j,1}) \beta_{k_2, n}^{(p)}(v_{j,2}) \beta_{k_3, n}^{(p)}(v_{j,3}), \quad \mathbf{k} = 0, \dots, N - 1,$$

where $\mathbf{v}_j = (v_{j,1}, v_{j,2}, v_{j,3})$ and $\beta_{r, n}^{(p)}(x) = 2^{-\frac{n}{2}} \beta^{(p)}(2^{-n}x - r)$ with $\beta^{(p)}$ being the central B -spline of order p . The computational cost of this step is $O(p^3 N_v)$.

Then we evaluate a trigonometric sum

$$F_l = \sum_{\mathbf{k}=0}^{N-1} g_k e^{2\pi i(\mathbf{k}, \mathbf{l})/N}, \quad \mathbf{l} = -N/2, \dots, N/2 - 1$$

using standard FFT algorithm with the cost $O(N^3 \log N)$.

The last step is the scaling of the Fourier transform F_l according to the formula:

$$\hat{f}_{\mathbf{m}} = \frac{1}{N^{\frac{3}{2}} \sqrt{a^{(p)}(m_1/N) a^{(p)}(m_2/N) a^{(p)}(m_3/N)}} F_{\mathbf{m}}, \quad \mathbf{m} = -M, \dots, M - 1,$$

where $a^{(p)}(m_j/N) = \sum_{l=-p}^p \beta^{(2p+1)}(l) e^{2\pi i l m_j / N}$. This step requires only $O(N^3)$ multiplications, hence the total cost of the USFFT algorithm can be estimated as $O(p^3 N_v) + O(N^3 \log N)$. The precision of these computations depends on the order p of the central B -splines $\beta^{(p)}$.

A similar procedure is used to calculate the inverse Fourier transform (7) which, discretized in the Fourier domain, is given by

$$f(\mathbf{v}) = \sum_{\mathbf{m}=-M}^{M-1} \hat{f}_{\mathbf{m}} e^{-2\pi i(\mathbf{m}, \mathbf{v})}, \quad \mathbf{v} \in \Omega_v. \tag{13}$$

Namely, we start with extending the Fourier coefficients

$$g_k = \begin{cases} \hat{f}_{k+M} & \text{if } -M \leq k \leq M - 1, \\ 0 & \text{otherwise,} \end{cases} \quad \mathbf{k} = -N/2, \dots, N/2 - 1.$$

Then we scale g_k according to the formula $\tilde{g}_k = \frac{g_k}{b_{k_1} b_{k_2} b_{k_3}}$, where $\hat{b}_{k_j} = \sum_{l=-\frac{p-1}{2}}^{\frac{p-1}{2}} \beta^{(p)}(l) e^{2\pi i l k_j / N}$. Next we apply the FFT algorithm to compute the sum

$$f_l = \sum_{\mathbf{k}=-N/2}^{N/2-1} \tilde{g}_k e^{2\pi i(\mathbf{l}, \mathbf{k})/N}, \quad \mathbf{l} = -N/2, \dots, N/2 - 1.$$

Finally, we evaluate f at any point $\mathbf{v} \in \Omega_v$ using the formula

$$f(\mathbf{v}) = \sum_{\mathbf{l}=-N/2}^{N/2-1} f_l \beta^{(p)}\left(\frac{N}{2} v_1 - l_1\right) \beta^{(p)}\left(\frac{N}{2} v_2 - l_2\right) \beta^{(p)}\left(\frac{N}{2} v_3 - l_3\right).$$

The cost of the first two steps of the algorithm is $O(N^3 \log N)$. The cost of the last step depends on the number of required computations of f in the velocity domain and for N_v points it is $O(p^3 N_v)$. Hence the total cost of calculation of the inverse Fourier transform is the same as before.

2.3. Gain and loss terms

Discretization of the collision operator $Q(f, f)$ is splitted according to (2) into three steps: computation of $Q_R^+(f, f)$, computation of $q_R^-(f)$ and pointwise multiplication of f and $q_R^-(f)$ in the points of the adaptive grid.

We start with the regularized gain term $Q_R^+(f, f)$ (cf. (8)), which is discretized as follows:

$$Q_R^+(f, f)(\mathbf{v}) = \sum_{\mathbf{l}, \mathbf{m}=-M}^{M-1} \hat{f}_{\mathbf{l}} \hat{f}_{\mathbf{m}} \hat{B}_R(\mathbf{l}, \mathbf{m}) e^{-2\pi i(\mathbf{l}+\mathbf{m}, \mathbf{v})}.$$

Using new indices $\mathbf{p} = \mathbf{l} + \mathbf{m}$ and $\mathbf{q} = \mathbf{l} - \mathbf{m}$ we change the summation to get

$$Q_R^+(f, f)(\mathbf{v}) = \sum_{\mathbf{p}} \sum_{\mathbf{q}} \hat{f}_{\frac{\mathbf{p}+\mathbf{q}}{2}} \hat{f}_{\frac{\mathbf{p}-\mathbf{q}}{2}} T(|\mathbf{p}|, |\mathbf{q}|) e^{-2\pi i(\mathbf{p}, \mathbf{v})},$$

where we use the fact that \hat{B}_R depends only on $|\mathbf{l} + \mathbf{m}|$ and $|\mathbf{l} - \mathbf{m}|$ in the VHS model (see [23]), thus we can define $T(|\mathbf{p}|, |\mathbf{q}|) := \hat{B}_R(\mathbf{l}, \mathbf{m})$.

We introduce the notation $F(\mathbf{p}) = \sum_{\mathbf{q}} \hat{f}_{\frac{\mathbf{p}+\mathbf{q}}{2}} \hat{f}_{\frac{\mathbf{p}-\mathbf{q}}{2}} T(|\mathbf{p}|, |\mathbf{q}|)$ and compute $F(\mathbf{p})$ for every \mathbf{p} with a cost $O(N^6)$. Then $Q_R^+(f, f)$ is an inverse Fourier transform of $F(\mathbf{p})$:

$$Q_R^+(f, f)(\mathbf{v}) = \sum_{\mathbf{p}} F(\mathbf{p}) e^{-2\pi i(\mathbf{p}, \mathbf{v})}$$

and must be computed in the points \mathbf{v} from the adaptive grid, in fact during the process when this grid is generated and in parallel to the computation of the solution f at the new time step. Because of this reason we use again the USFFT by Beylkin [2] here, now its inverse version, to compute $Q_R^+(f, f)$ effectively and independently for each \mathbf{v} point in the grid.

The discretization of the loss term $Q_R^-(f, f)$ consists of the computation of the discrete collision frequency term (cf. (9))

$$q_R^-(f)(\mathbf{v}) = \sum_{\mathbf{m}=-M}^{M-1} \hat{f}_{\mathbf{m}} \widehat{B}_R(\mathbf{m}, \mathbf{m}) e^{-2\pi i(\mathbf{m}, \mathbf{v})},$$

which is a convolution operator and a pointwise multiplication of $q_R^-(f)(\mathbf{v})$ by $f(\mathbf{v})$. We compute $q_R^-(f)(\mathbf{v})$ again using USFFT algorithm. The total computational cost of the numerical approximation of the collision operator is $O(N_v) + O(N^6 \log N)$.

We point out that the computational cost consists of two parts. The first one depends on the approximation of the discontinuous solution and increases linearly with the number N_v of the points in the adaptive velocity grid. Another part depends on the number N of Fourier modes along one coordinate direction, i.e. on the approximation of the smooth terms $Q_R^+(f, f)$ and $q_R^-(f)$ in the Boltzmann equation.

3. Time discretization

The homogeneous Boltzmann equation is solved numerically using either the standard semi-implicit Euler scheme

$$\tilde{f}^{n+1} = \frac{f^n + \Delta t Q^+(f^n, f^n)}{1 + \Delta t q^-(f^n)} \tag{14}$$

or the second order Runge–Kutta scheme

$$\tilde{f}^{n+1} = f^n + \frac{\Delta t}{2} (K_1 + K_2), \tag{15}$$

where $f^n = f(t_n)$ denotes the solution f at time t_n and $K_1 = Q(f^n, f^n)$, $K_2 = Q(f^n + K_1, f^n + K_1)$.

The proposed numerical scheme conserves only mass (spectral methods do not represent higher moments of solutions exactly), momentum and energy are not conserved. We use here a correction technique which enforces the conservation and was proposed by Aristov and Tcheremisin [1]. The numerical solution \tilde{f}^{n+1} given by (14) or (15) is corrected by multiplying by a polynomial

$$1 + \sum_{i=0}^4 \alpha_i \psi_i,$$

where $\psi_0(\mathbf{v}) = 1$, $\psi_i(\mathbf{v}) = v_i$ for $i = 1, 2, 3$ and $\psi_4(\mathbf{v}) = |\mathbf{v}|$. The numbers α_i are determined by requiring that the (discretized) conservation laws

$$\sum_{\mathbf{v}_j \in \mathcal{G}_v} \psi_l(\mathbf{v}_j) \tilde{f}^{n+1}(\mathbf{v}_j) \left(1 + \sum_{i=0}^4 \alpha_i \psi_i(\mathbf{v}_j) \right) = \sum_{\mathbf{v}_j \in \mathcal{G}_v} \psi_l(\mathbf{v}_j) f^n(\mathbf{v}_j)$$

are satisfied for $l = 0, \dots, 4$. Hence we get the following formula for the solution:

$$f^{n+1} = \tilde{f}^{n+1} \left(1 + \sum_{i=0}^4 \alpha_i \psi_i \right). \tag{16}$$

At each time step a new adaptive grid is built for the solution f^{n+1} according to the algorithm presented in Section 2.1.

4. Numerical examples

In this section, we present the numerical tests and examples showing the effectiveness of our method. We start with classical tests where we compare the results of our method with the analytical BKW solution and with the results of DSMC method for the gas of hard spheres. Next we illustrate our method by two examples with discontinuous initial data.

4.1. Continuous initial data

Test 1. In this test we compare our method with the classical BKW analytical solution to the Boltzmann equation in the case of Maxwell molecules (cf. [6,15]). At each time step we compute the relative L_1 and L_2 norms of the error of the numerical solution according to the formula:

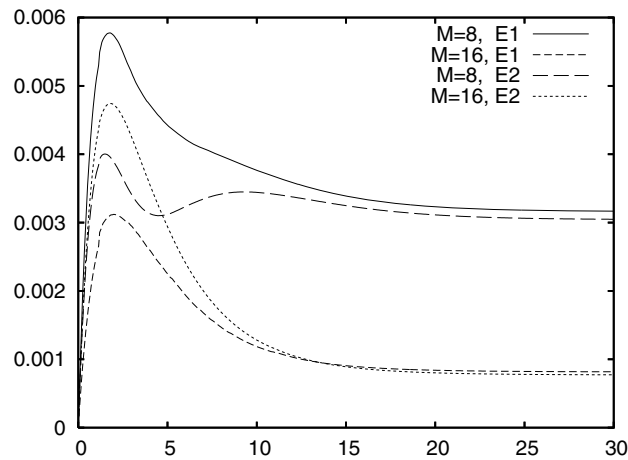


Fig. 2. Relative L_1 and L_2 norms of errors of the BKW solution.

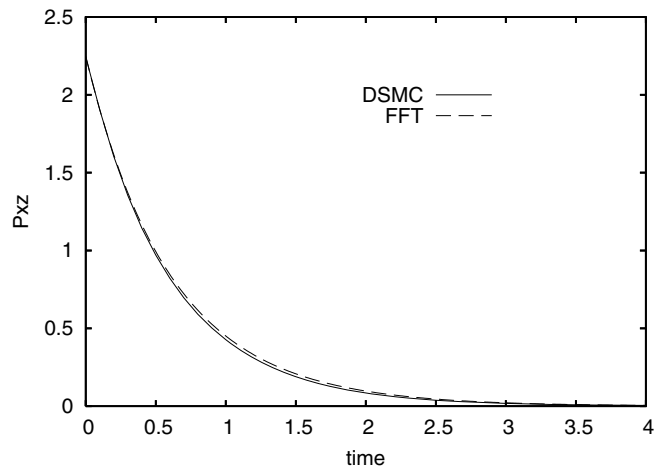


Fig. 3. Relaxation of xz -moment.

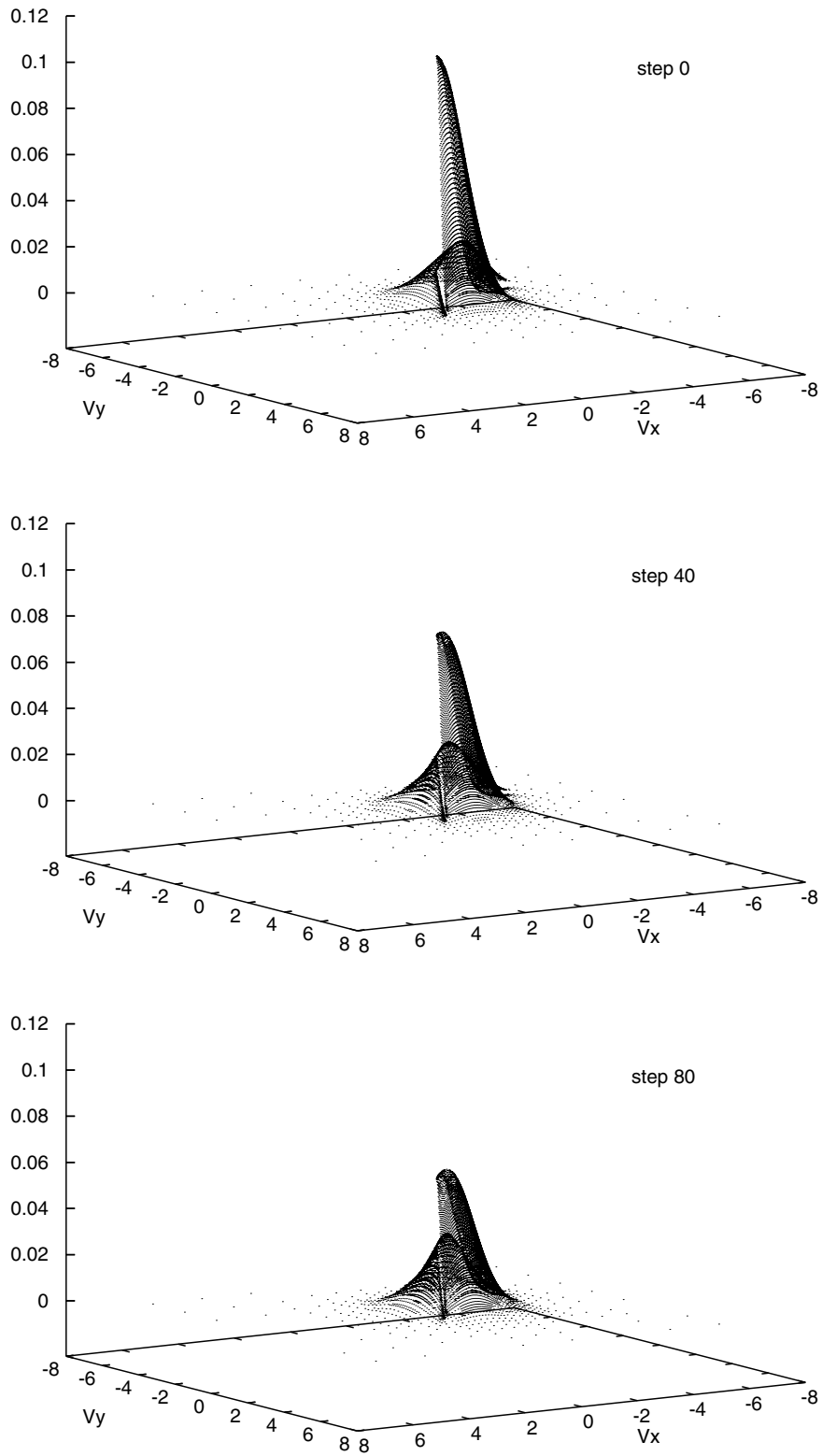


Fig. 4. Example 1, solution steps 0, 40 and 80.

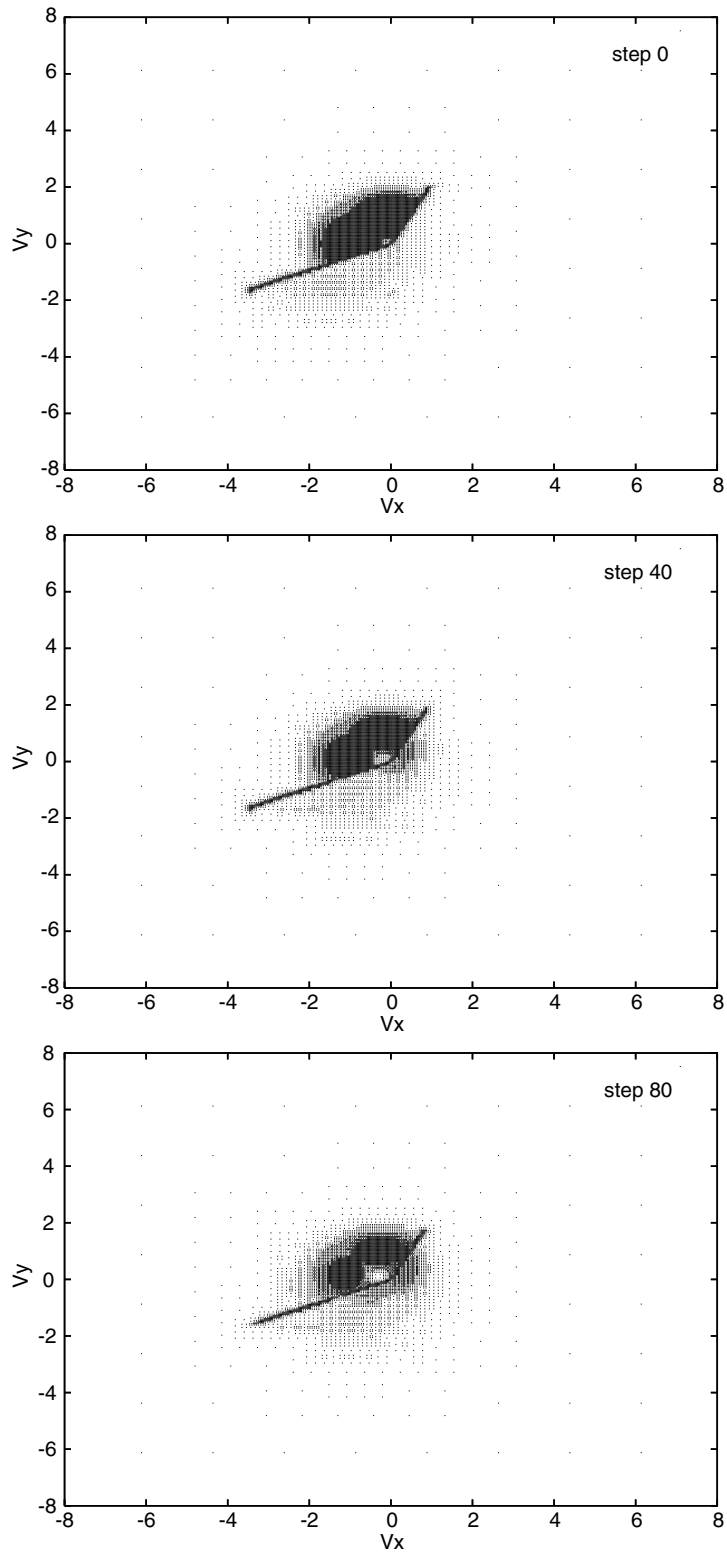


Fig. 5. Example 1, grid steps 0, 40 and 80.

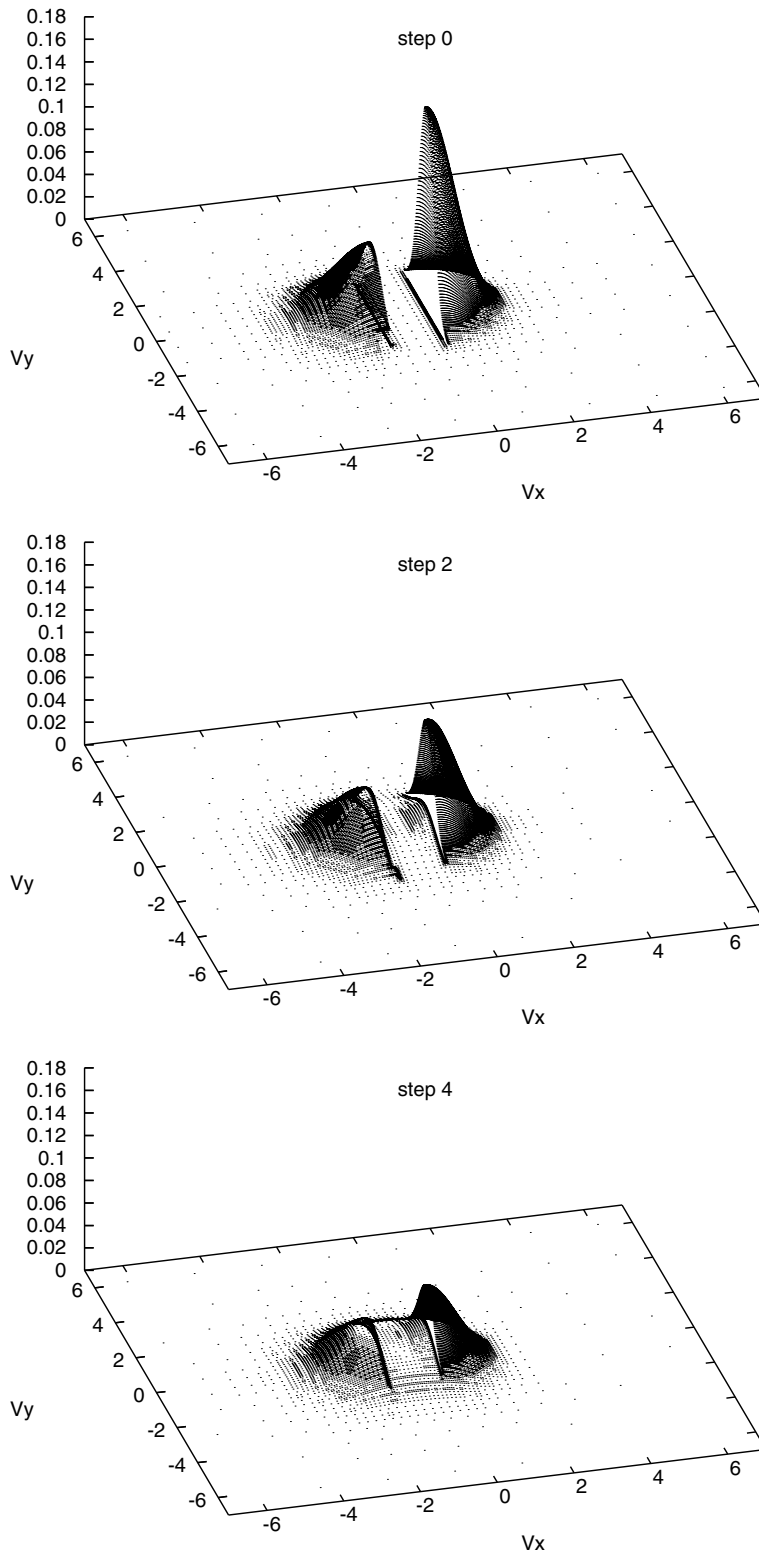


Fig. 6. Example 2, solution steps 0, 2 and 4.

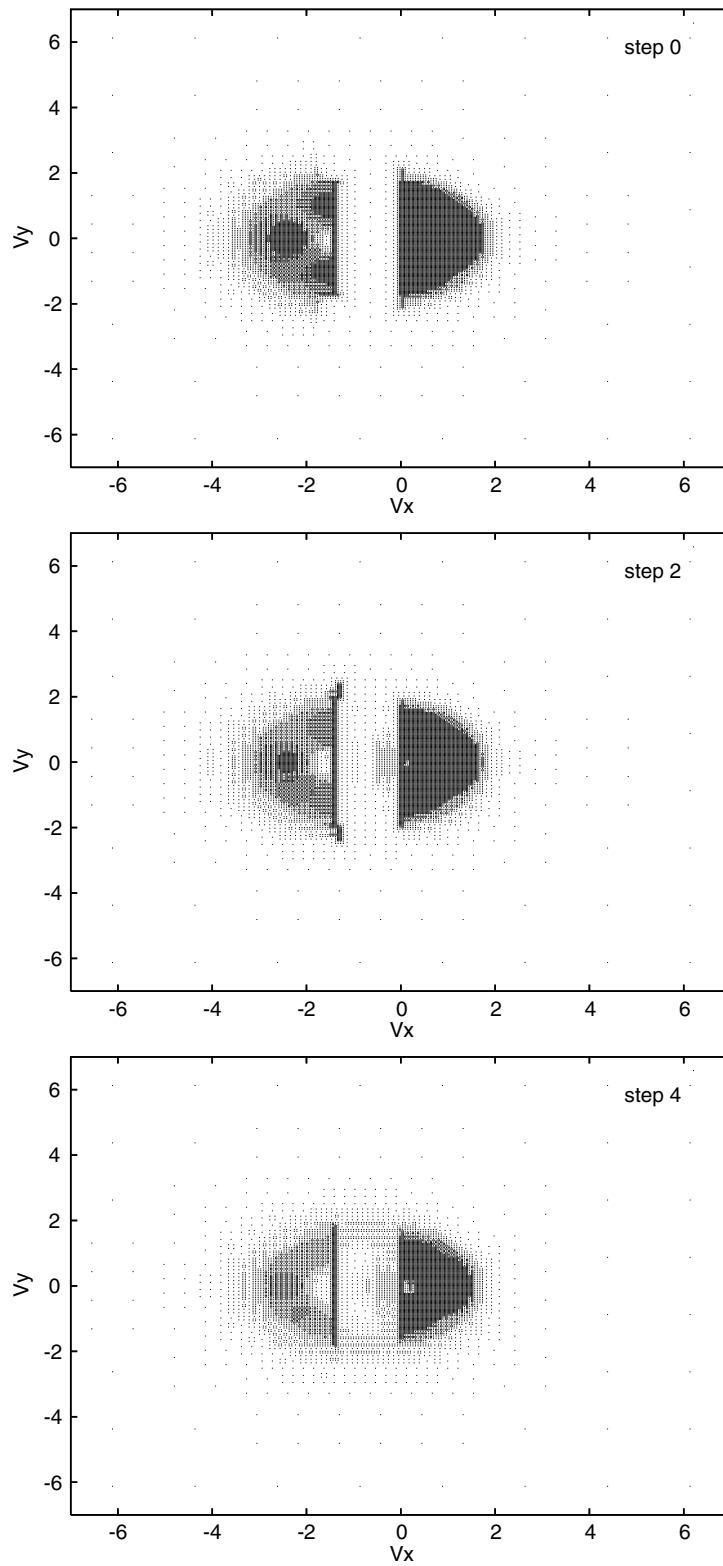


Fig. 7. Example 2, grid steps 0, 2 and 4.

$$E_p = \frac{\|f^h(t) - f(t)\|_p}{\|f(t)\|_p},$$

where $\|\cdot\|_p$ with $p = 1$ or $p = 2$ denotes the corresponding L_p norm and $f^h(t)$ and $f(t)$ are the numerical and analytical solutions at time t . Fig. 2 shows the computed norms for the parameters $M = 8$ and $M = 16$ (i.e. the number of Fourier modes in one direction is $2M = 16$ and $2M = 32$, respectively). The computations were performed using the second order Runge–Kutta scheme for the time step $\Delta t = 0.12$.

Test 2. In the second test we give the results for a relaxation problem in the case of hard sphere molecules and compare them with the solution obtained by the DSMC method (cf. [14]).

We study the relaxation process of the second moment of solution of the Boltzmann equation. As the initial data we take the sum of two Maxwellian functions:

$$f_0(\mathbf{v}) = \frac{1}{2(2\pi T)^{3/2}} \left[\exp\left(-\frac{|\mathbf{v} - \mathbf{u}|^2}{2T}\right) + \exp\left(-\frac{|\mathbf{v} + \mathbf{u}|^2}{2T}\right) \right]$$

with $\mathbf{u} = (1.5, 0, 1.5)$ and $T = 0.5$. In Fig. 3, we present the relaxation of the second moment in xz -direction. The computation was performed using the Runge–Kutta scheme with time step $\Delta t = 0.02$ and for $M = 8$.

4.2. Discontinuous initial data

Having in mind future applications of our approach to boundary value problems we chose data with discontinuities typical for flows around bodies. We use the model of Maxwell pseudo-molecules in Example 1 and hard sphere molecules in Example 2. In both examples below the Maxwell distribution function has the form $f_M(\mathbf{v}) = \frac{1}{(2\pi T)^{3/2}} e^{-|\mathbf{v} - \mathbf{u}|^2/2T}$.

Example 1. In the first example (see Figs. 4 and 5) the initial distribution function imitates the distribution function in the gas flow around a sphere at a point x at some finite distance from the sphere. It is initially equal to the Maxwell distribution function with $T = 0.7$ and $\mathbf{u} = (0, 0, 0)$ for points within a cone with centre at the origin. Outside of this cone the initial distribution function is taken equal to another Maxwell distribution with $T = 1.7$ and $\mathbf{u} = (-1.5, 0, 0)$. The cone has the axis laying in $v_x - v_y$ plane with an angle of 135° with respect to the v_x -axis. The angle α between the cone and its axis is 75° . The computation was performed using the Runge–Kutta scheme with time step $\Delta t = 0.02$ for $M = 8$ and the number of points in the adaptive velocity grid was of the order of 10^6 .

Example 2. The second example (see Figs. 6 and 7) is given to illustrate the method on solutions with discontinuities along planes. The initial distribution function is a Maxwell distribution function with $T = 1.0$ and $\mathbf{u} = (0, 0, 0)$ in the half space $v_x > 0$ and is another Maxwell distribution with $T = 0.5$ and $\mathbf{u} = (-1.4, 0, 0)$ in the half space $v_x < -1.4$. There are no particles within a gap with velocities with $-1.4 < v_x < 0$. The computation was performed using the Runge–Kutta scheme with time step $\Delta t = 0.02$ for $M = 8$ and the number of points in the adaptive velocity grid was of the order of 10^6 .

Each of these examples is illustrated by a sequence of graphs for values of the distribution function $f(t_i, \mathbf{v})$ for several time points $t_i = 0.02 * i$ in $v_x - v_y$ plane (Figs. 4 and 6) and also the corresponding cross-sections of the three-dimensional adaptive grid with $v_x - v_y$ plane (Figs. 5 and 7). The numerical results show that the initial discontinuity in the distribution function decreases but preserves its position in complete accordance with the known properties of the Boltzmann equation, see [18].

5. Conclusions

In the present paper we have developed a new fast numerical method for computing discontinuous solutions to the Boltzmann equation. The method uses an adaptive grid for solutions for effective resolution of the discontinuous distribution function. The Fourier spectral representation is used for the gain term and for the collision frequency that are known to be regular terms in the equation [16,27,18]. An approximate fast

Fourier transform on the non-uniform grid makes it possible to do the fast computation of the gain term and the collision frequency on the adaptive grid.

The comparisons to the DSMC scheme for hard sphere molecules and to the analytical BKW solution show very good agreement even for rather small number of Fourier modes. The effectiveness of the method in the case of discontinuous initial data is verified by numerical tests.

In the present paper we discuss the method for the homogeneous Boltzmann equation. Some strategies to deal with space non-uniform problems are currently under development and the results will be described elsewhere.

References

- [1] V.V. Aristov, F.G. Tcheremisin, The conservative splitting method for the solution of a Boltzmann equation, *Zh. Vychisl. Mat. i Mat. Fiz.* 20 (1) (1980) 191–207, 262.
- [2] G. Beylkin, On the fast Fourier transform of functions with singularities, *Appl. Comput. Harmon. Anal.* 2 (4) (1995) 363–381.
- [3] G.A. Bird, *Molecular Gas Dynamics and the Direct Simulation of Gas Flows*, Oxford Engineering Science Series, vol. 42, Clarendon Press, Oxford, 1994.
- [4] G.A. Bird, Recent advances and current challenges for DSMC, *Comput. Math. Appl.* 35 (1–2) (1998) 1–14, simulation methods in kinetic theory.
- [5] A. Bobylev, S. Rjasanow, Difference scheme for the Boltzmann equation based on the fast Fourier transform, *Eur. J. Mech. B: Fluids* 16 (2) (1997) 293–306.
- [6] A.V. Bobylev, Exact solutions of the Boltzmann equation, *Dokl. Akad. Nauk SSSR* 225 (6) (1975) 1296–1299.
- [7] A.V. Bobylev, The method of the Fourier transform in the theory of the Boltzmann equation for Maxwell molecules, *Dokl. Akad. Nauk SSSR* 225 (6) (1975) 1041–1044.
- [8] A.V. Bobylev, S. Rjasanow, Fast deterministic method of solving the Boltzmann equation for hard spheres, *Eur. J. Mech. B: Fluids* 18 (5) (1999) 869–887.
- [9] C. Buet, A discrete-velocity scheme for the Boltzmann operator of rarefied gas dynamics, *Transport Theory Statist. Phys.* 25 (1) (1996) 33–60.
- [10] C. Cercignani, *The Boltzmann Equation and its Applications*, Applied Mathematical Sciences, vol. 67, Springer-Verlag, New York, 1988.
- [11] E. Gabetta, L. Pareschi, The Maxwell gas and its Fourier transform towards a numerical approximation, in: *Waves and Stability in Continuous Media* (Bologna, 1993), Ser. Adv. Math. Appl. Sci., World Scientific Publishing, River Edge, NJ, 1994, pp. 197–201.
- [12] D. Goldstein, B. Sturtevant, J. Broadwell, Investigation of the motion of discrete-velocity gases, in: E.P. Muntz et al. (Eds.), *Proceedings of the 16th International Symposium on RGD*, Ser. Progress in Astronautics and Aeronautics, vol. 118, 1989, pp. 100–117.
- [13] S. Kosuge, K. Aoki, S. Takata, Shock-wave structure for a binary gas mixture: finite-difference analysis of the Boltzmann equation for hard-sphere molecules, *Eur. J. Mech. B: Fluids* 20 (1) (2001) 87–101.
- [14] P. Kowalczyk, A. Palczewski, G. Russo, Z. Walenta, Numerical solutions of the Boltzmann equation: comparison of different algorithms, *Eur. J. Mech. B: Fluids* 27 (1) (2008) 62–74, doi:10.1016/j.euromechflu.2007.04.001.
- [15] M. Krook, T.T. Wu, Exact solutions of the Boltzmann equation, *Phys. Fluids A* 20 (10) (1977) 1589–1595.
- [16] P.-L. Lions, Compactness in Boltzmann's equation via Fourier integral operators and applications. I, II, *J. Math. Kyoto Univ.* 34 (2) (1994) 391–427, 429–461.
- [17] S. Mischler, Convergence of discrete-velocity schemes for the Boltzmann equation, *Arch. Ration. Mech. Anal.* 140 (1) (1997) 53–77.
- [18] C. Mouhot, C. Villani, Regularity theory for the spatially homogeneous Boltzmann equation with cut-off, *Arch. Ration. Mech. Anal.* 173 (2) (2004) 169–212.
- [19] T. Ohwada, Structure of normal shock waves: direct numerical analysis of the Boltzmann equation for hard-sphere molecules, *Phys. Fluids A* 5 (1) (1993) 217–234.
- [20] A. Palczewski, J. Schneider, A.V. Bobylev, A consistency result for a discrete-velocity model of the Boltzmann equation, *SIAM J. Numer. Anal.* 34 (5) (1997) 1865–1883.
- [21] V.A. Panferov, A.G. Heintz, A new consistent discrete-velocity model for the Boltzmann equation, *Math. Methods Appl. Sci.* 25 (7) (2002) 571–593.
- [22] L. Pareschi, B. Perthame, A Fourier spectral method for homogeneous Boltzmann equations, in: *Proceedings of the Second International Workshop on Nonlinear Kinetic Theories and Mathematical Aspects of Hyperbolic Systems* (Sanremo, 1994), 1996.
- [23] L. Pareschi, G. Russo, Numerical solution of the Boltzmann equation. I. Spectrally accurate approximation of the collision operator, *SIAM J. Numer. Anal.* 37 (4) (2000) 1217–1245 (electronic).
- [24] S. Rjasanow, W. Wagner, *Stochastic numerics for the Boltzmann equation*, Springer Series in Computational Mathematics, vol. 37, Springer, Berlin, 2005.
- [25] F. Rogier, J. Schneider, A direct method for solving the Boltzmann equation, *Transport Theory Statist. Phys.* 23 (1–3) (1994) 313–338.

- [26] S. Takata, Y. Sone, K. Aoki, Numerical analysis of a uniform flow of a rarefied gas past a sphere on the basis of the Boltzmann equation for hard-sphere molecules, *Phys. Fluids A* 5 (3) (1993) 716–737.
- [27] B. Wennberg, The geometry of binary collisions and generalized Radon transforms, *Arch. Ration. Mech. Anal.* 139 (3) (1997) 291–302.